Sensing and Bio-Sensing Research 51 (2026) 100941

Contents lists available at ScienceDirect

Sensing and Bio-Sensing Research

journal homepage: www.elsevier.com/locate/sbsr

Microfluidic Padlock Probe-based Rolling Circle Amplification for sensitive detection of *mecA* resistance gene in *Staphylococcus aureus*☆

Léo Baldenweck [a], Catarina Caneira [b,c], Jasmina Vidic [a,*]

[a] Université Paris-Saclay, Institut Micalis, INRAE, AgroParisTech, Jouy-en-Josas, France
[b] Instituto de Engenharia de Sistemas e Computadores – Microsistemas e Nanotecnologias (INESC MN), Lisboa, Portugal
[c] Associate laboratory i4HB-Institute for Health and Bioeconomy et INESC, MN, Lisboa, Portugal

ARTICLE INFO

Keywords:
Staphylococcus aureus
mecA gene
Padlock probe
Rolling circle amplification
Fluorescent biosensor

ABSTRACT

Antimicrobial resistance and the dissemination of resistance genes remain critical global health challenges, demanding efficient monitoring and detection tools. Methicillin-resistant *Staphylococcus aureus* (MRSA) is a prominent example, posing serious clinical and epidemiological concerns. Here, we developed a sensitive detection platform combining isothermal Padlock Probe-based Rolling Circle Amplification with a bead-based microfluidic biosensor and fluorescent readout for the detection of the *mecA* gene in *S. aureus*. The assay design was first validated using a complementary synthetic ssDNA target, then optimized with genomic dsDNA extracted from a laboratory strain. The optimized system was subsequently applied to clinical isolates from sepsis cases and complex matrices simulating natural habitats, including milk, serum, and salad. The biosensor achieved a detection limit of 10^4 cells with 100 % specificity compared to PCR at an analysis time of two hour. All reaction steps were carried out sequentially within the microfluidic device, highlighting the strong potential of the device for full automation and for extension to additional bacterial genes.

1. Introduction

Bacterial infections are a leading cause of mortality and morbidity worldwide, responsible for an estimated 13.6 % of all global deaths in 2019 [18]. A recent study estimated that 4.71 million deaths in 2021 were linked to bacterial antimicrobial resistance (AMR), with *Staphylococcus aureus* showing the highest annual increase in attributable deaths among significant pathogens [27].

S. aureus is an opportunistic Gram-positive bacterium that colonizes humans, animals, and the environment. It typically forms grape-like clusters and spreads through contact with infected individuals, contaminated surfaces, animals, food and water [17,23]. Its virulence is attributed to a wide range of virulence factors enabling host colonization, immune system evasion, and causing tissue damage. Its adaptive fitness drives partial or full resistance to previously effective antimicrobial agents. Notably, methicillin-resistant *S. aureus* (MRSA) presents significant public health challenges. Methicillin, a β-lactam antibiotic, blocks cell wall synthesis by interacting with the Penicillin-Binding-Protein (PBP) [10]. The resistance is attributed to the production of a modified PBP, PBP2a, which has a reduced affinity for β-lactam antibiotics [2,31].

The synthesis of the altered PBP2a is enabled by the presence of a mobile genetic element, the staphylococcal cassette chromosome mec (SCCmec), which carries the *mecA* gene [22]. Bacteria harboring this cassette exhibit resistance to β-lactam antibiotics, including methicillin, cefoxitin, and oxacillin [33]. The gold standard for detecting AMR is the susceptibility test. The method is based on the phenotypical response of the bacteria to the given antibiotics, and provides results in 1–3 days. During this period, the patient is usually treated with a broad-spectrum antibiotic, a practice that favors the emergence of additional resistance [3]. Besides, the antibiotic susceptibility test may fail to provide accurate results if the patient is already receiving antibiotic treatment.

Genotyping is commonly performed as a secondary test to confirm the results of the susceptibility test. The Polymerase Chain Reaction (PCR), which specifically and exponentially amplifies target DNA, is used in most cases, but microarray or genome sequencing may also be performed [29,32,40]. Those methods allow detection in hours or a day but require laborious and time-consuming target identification strategies (gel electrophoresis or amplicon sequencing), are costly and need specific materials and trained staff, which place significant obstacles to a

☆ This article is part of a Special issue entitled: 'Biosensors 2025' published in Sensing and Bio-Sensing Research.

* Corresponding author.
E-mail address: jasmina.vidic@inrae.fr (J. Vidic).

https://doi.org/10.1016/j.sbsr.2025.100941
Received 31 October 2025; Received in revised form 3 December 2025; Accepted 9 December 2025
Available online 11 December 2025

wide application [11]. Moreover, PCR-based methods can be inhibited by compounds present in biological matrices, such as hemoglobin, immunoglobulins and myoglobin in blood [1,35] or complex polysaccharides, metal ions, and nucleases in food and environmental samples [14].

To address PCR drawbacks, isothermal amplification methods have been developed to detect nucleic acid biomarkers accurately, enabling faster amplification. They eliminate the need for temperature changes or skilled personnel [40]. Among them, Padlock Probe-based Rolling Circle Amplification (RCA) offers high potential for clinical diagnosis and surveillance of AMR spreading. It provides rapid, enhanced amplification, simple operation, and easy amplicons detection. The method bypasses the need for thermal cycling, reducing equipment and turnaround time. In contrast to other isothermal amplification methods, such as loop-mediated isothermal amplification (LAMP) which runs at ~65 °C [12], RCA operates at 37 °C. This makes RCA more energy-efficient and sustainable option.

Padlock Probe-mediated RCA employs a specific single-stranded DNA, named Padlock, that becomes circularized in the presence of the target sequence. This circular structure enables amplification, which can be monitored in real time when the probe is coupled with a fluorescent beacon reporter. The reaction was first described in 1994 by Nilsson et al. [28], and since then, it has been used for the detection of microRNA [20,24], mRNA [39], extracellular vesicles [15], and viruses and bacteria [7,26,39]. These reports suggest that Padlock Probe-RCA may serve as an efficient portable tool for AMR surveillance workflows. Nonetheless, challenges remain in standardization, multiplexing capabilities, and ensuring specificity in complex biological fluids, especially when the target gene is in doubled strained genomic DNA (gDNA).

Currently, microfluidic chips have attracted extensive attention for their versatile applications in biomedical testing, environmental monitoring, and other interdisciplinary fields. These lab-on-a-chip devices rely on the manipulation of fluids within channels that have dimensions on the order of tens to hundreds of micrometers [6,9]. They can integrate sample preparation, reaction, washing, and detection processes at the microscale. This reduction in the volume of reagents and analytes enables device miniaturization and reduces both the cost and duration of analyses. Additionally, the miniaturization and simplification of microfluidic fluorescence systems combined with smartphone-based colour recognition hold great potential for point-of-care applications [37].

In this study, we developed a microfluidic-based Padlock Probe-RCA using streptavidin beads and a fluorescent read-out for the detection of the *mecA* gene in *S. aureus* genomic DNA (gDNA). The applicability of the biosensor was confirmed on *S. aureus* clinical isolates with 100 % specificity (benchmarked against PCR). In addition, the high sensitivity and specificity were demonstrated using *S. aureus* cells spiked to natural bacterial biotopes: milk, serum and green salad.

2. Experimental section

2.1. Bacterial strains and growth conditions

Two lab strains of *S. aureus* were used for method development and optimization: *S. aureus* USA300-JE2 (JE2) which is methicillin-resistant and *mecA* positive [13], and *S. aureus* RN-R strain which is methicillin-susceptible and harbors no SCCmec [30]. Ten clinical *S. aureus* strains used were blood isolates from anonymized patients collected during sepsis diagnostic procedures. They were kindly provided by Prof. Jean-Louis Herrmann from Raymond Poincaré Hospital, Garches, France. Bacteria were routinely cultivated overnight in Brain Heart Infusion (BHI) broth at 37 °C with agitation at 180 rpm.

2.2. Genomic DNA extraction

S. aureus overnight culture was washed with TES buffer (10 mM Tris-HCl, 100 mM NaCl, 1.0 mM EDTA, pH of 7.8). The pellet was lysed using the FastPrep-24 kit (MP Biomedicals, France) with three cycles of 20 s at speed 4 m/s, with 5 min rest between each cycle. Lysates were clarified by centrifugation at 8000 *g* for 10 min at 4 °C. The gDNA was purified using the DNeasy blood and tissue kit (Qiagen, France) following the manufacturer's instructions. Concentration of gDNA (ng/µl) was determined by NanoDrop2000 (ThermoScientific, France). The number of *mecA* gene copies was calculated using the website NEBioCalculator from Biolabs with the following formula:

$$\textit{mecA}\ \text{DNA copy number} = \left(\frac{\text{mass of DNA (g)}}{\text{length of dsDNA(bp)} \times \frac{615.96\left(\frac{\text{g}}{\text{mol}}\right)}{\text{(bp)}} + 36.04\left(\frac{\text{g}}{\text{mol}}\right)} \right) \times 6.022 \times 10^{23} \left(\frac{\text{molecules}}{\text{mol}}\right) \quad (1)$$

As *mecA* is a single-copy gene in the genome of *S. aureus*, we can approximate that one *mecA* DNA copy corresponds to one Colony Forming Unit (CFU).

2.3. Design of padlock probe and PCR primers

The DNA oligos were designed based on the *mecA* sequence extracted from *S. aureus* JE2 (NCBI accession number: NZ_CP020619), and on verification of sequence conservation among other MRSA strains. PCR primers mecAF and mecAR were designed using Primer3 from Benchling (https://benchling.com). Padlock Probe was designed according the guideline of Krishnan, Soares, Madaboosi, and Gromiha [21]. Both primers and Padlock specificity were tested with Basic Local Alignment Search Tool (BLAST) on NCBI. All sequences are presented in Table S1 and were synthesized by Eurofins Genomics.

2.4. Construction of microfluidic device

The microchannel designs were created using AutoCAD 2024 software (version 24.3) (Autodesk, San Francisco, CA, USA) as described before [7]. To generate the aluminum hard masks, the design pattern was transferred to a Corning Eagle glass substrate with a 200 nm aluminum layer using direct-write laser lithography (Heidelberg DWLII, Heidelberg Instruments, Heidelberg, Germany), followed by etching with Gravure Aluminum Etchant (Microchemicals, Ulm, Germany).

To create microfluidic channels of 2 different heights, two aluminum hard masks were fabricated. Using these hard masks, an SU-8 master mold was manufactured using two different SU-8 photoresists, one for each height (SU-82015 for 20 µm, and SU-8 50 for 100 µm layers, both from Microchem, Newton, MA, USA). For each layer, the photoresist was spin-coated on a silicon wafer, exposed to UV light through the corresponding aluminum hard mask (UV KUB-2, KLOÉ, Saint-Mathieu-de-Tréviers, France) and baked. Following the baking, the unexposed

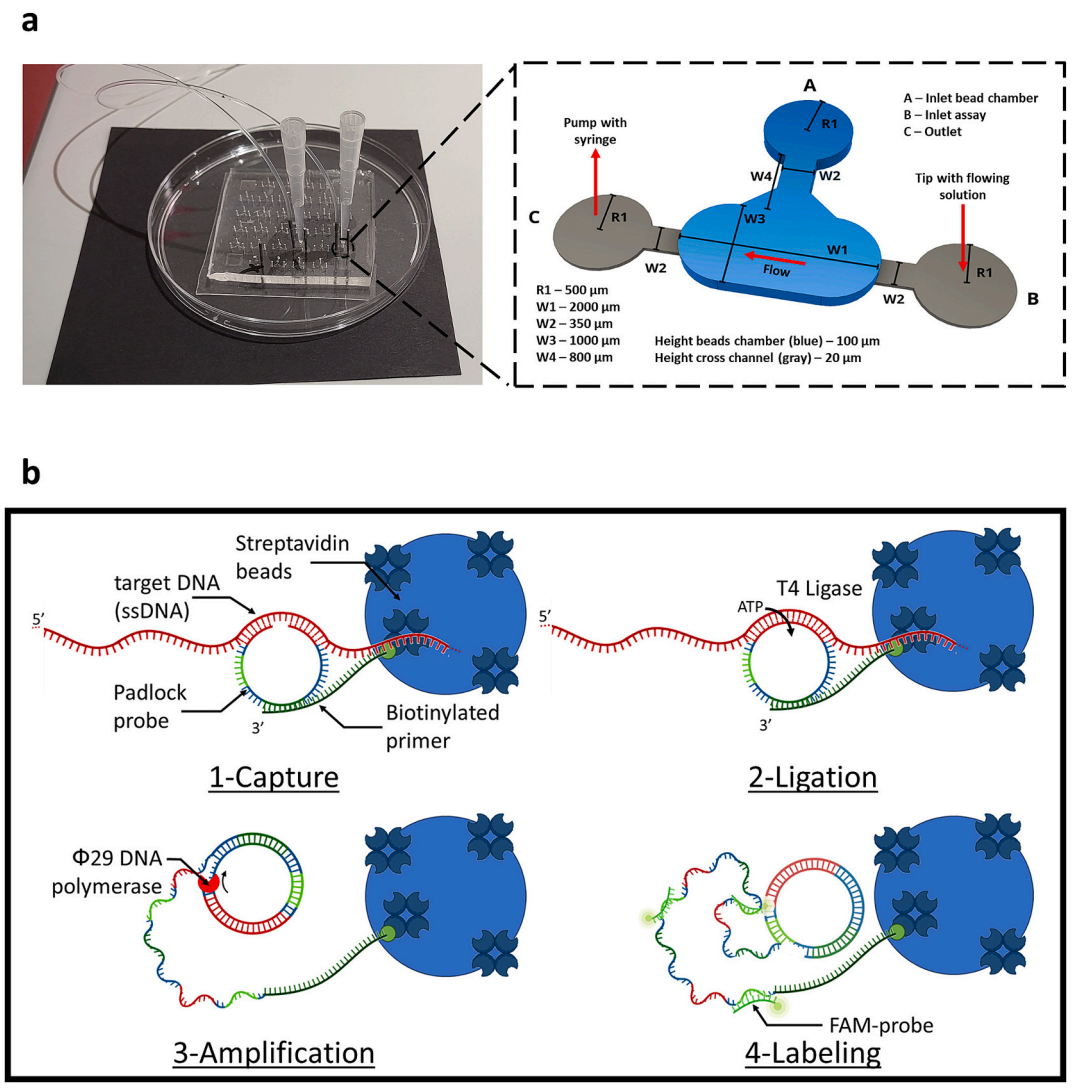

Fig. 1. Experimental setup and detection principle. (**a**) The microfluidic chip with 32 reaction chambers has tubing to the pump for continuous flow of solutions, as well as tips for injecting analytes and reagents. On the right, schematic illustration of one reaction chamber, which has three inlets: Inlet A for bead loading; Inlet B is the entrance of the chamber, connected to a tip containing the flowing solution; and Inlet C linked to the pump to exercise the negative pressure responsible for the flow and collect the waste solution. In blue is the bead chamber and in gray the cross channel. (**b**) Design of the Padlock Probe-based Rolling Circle Amplification sensor for the *mecA* gene. Step 1-Capture: The streptavidin from the beads interacts with the biotin from the primer. The Padlock Probe hybridizes with the 3′-end of the Biotin-primer, while its arms hybridize with the target *mecA* sequence. Step 2-Ligation: In the presence of the target gene, the T4 ligase catalyzes the formation of a phosphodiester bond between the 5′ phosphate and the 3′ hydroxyl termini of the Padlock Probe. Step 3-Amplification: Φ29 polymerase interacts with the primer and initiates the amplification of the Padlock Probe sequence. The polymerase's endonuclease activity will detach the target strand to continue polymerization, as with the primer. It results in a long ssDNA with multiple repetitions of the Padlock Probe sequence. Step 4-Labeling: The FAM-probe hybridizes with its complementary sequence in the backbone of the numerous repetitions of the Padlock Probes' complementary sequence that were amplified via Padlock Probe-RCA, targeting the *mecA* gene. (For interpretation of the references to colour in this figure legend, the reader is referred to the web version of this article.)

photoresist was removed with propylene glycol methyl ether acetate (PGMEA, 99.5 %, Sigma-Aldrich, St. Louis, MO, USA). To fabricate the PDMS (polydimethylsiloxane) structure, the Sylgard 184 silicon elastomer kit (Dow Corning, Midland, MI, USA) was used. The curing agent and base were mixed at a 1:10 (*w*/w) ratio and degassed. The mixture was then poured onto the SU-8 mold and covered with a flat poly (methyl methacrylate) (PMMA) frame and placed in the oven to cure at 70 °C for 90 min. Following this, the inlets and outlets of the structure were punctured using a 20 ga blunt needle (Instech Laboratories Inc., Plymouth Meeting, PA, USA). A PDMS slab (500 µm thick) is prepared by spin-coating the PDMS mixture on a silicon wafer and curing under the same conditions as aforementioned. Lastly, the PDMS slab and the microfluidic patterned PDMS were treated with oxygen plasma (1 min, high intensity; Harrick Plasma, Ithaca, NY, USA) and brought into conformal contact to establish an irreversible bond. The fabrication process is presented in Fig. S1.

2.5. Microfluidic assay

A 1 mL syringe was filled with phosphate-buffered saline (PBS) and mounted on a pump (NE-4000 Two Channel Programmable Syringe Pump, New Era Pump Systems Inc., USA) to deliver PBS. Using a polyethylene pipe (BTPE-60, from INSTECH, USA), the syringe was connected to the outlet C of one of the 32 chambers of the microfluidic device that was kept at 37 °C during the experiment (Fig. 1a and Fig. S2). The reaction chamber of the device was fully packed with Streptavidin Agarose Ultra Performance beads (Vectorlabs, USA) with a medium size of 35 µm at a flow rate of 4.5 µL/min by the inlet A. After loading, the inlet A was closed by a stainless-steel catheter plug. After this step, reaction solutions were flowed by the inlet B using a pipette tip (Fig. 1a).

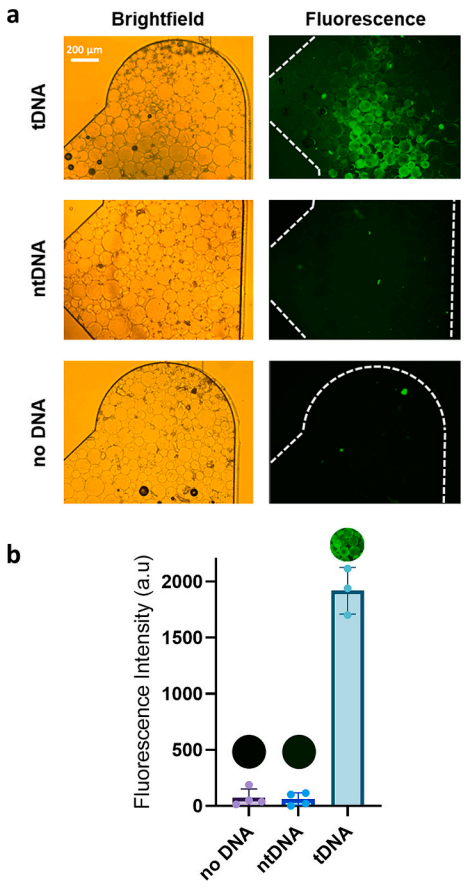

Fig. 2. Padlock Probe-RCA detection of the synthetic target ssDNA (**a**) Representative optical and fluorescent images acquired for microfluidic experiments performed with *mecA* target DNA (tDNA), control non-target DNA (ntDNA), and without DNA. Fluorescent images were acquired with a 5 s exposure time and a magnitude of 10×. (**b**) Intensity of the fluorescent signal obtained for different synthetic ssDNA, with a zoom of streptavidin beads observed close to the assay inlet for each condition to illustrate the selectivity of detection. Results represent the mean ± SD from at least three independent experiments.

To prevent nonspecific binding, the beads were washed with PBS, then saturated with 4 % BSA solution in PBS at 2 µL/min for 15 min. All solutions used were kept at 37 °C before their injection into the microfluidic device.

The Capture solution (0.175 µM Biotin-primer, 0.3 µM Padlock Probe, 10 µM target ssDNA, PBS) was flowed at 0.5 µL/min at 37 °C for 40 min. The Ligation solution (1 mM ATP, 0.04 % BSA, 1× T4 Buffer (Biolabs, Germany), 0.2 U/L T4 ligase (Biolabs, Germany), and milliQ water) was then flowed at 0.5 µL/min for 40 min. The Amplification solution (1× Φ29 DNA Polymerase Buffer (Biolabs, Germany), 0.05 % BSA, 0.4 mM of each dNTP (Biolabs, Germany), 0.5 U/L Φ29 polymerase (Biolabs, Germany) and milliQ water) was flowed at 0.25 µL/min for 60 min. The Labeling solution containing the hybridization buffer (1.4 M NaCl, 0.01 % TWEEN 20, 20 mM Tris-HCl, 5 mM EDTA, pH 8) and 0.5 µM detection DNA probe were flowed at 2 µL/min for 15 min. The channels were then washed with PBS, and protected from light with aluminum foil. For gDNA, the Capture solution was heated to 95 °C for 10 min to enable double strand DNA to open and then cooled in an ice bath for 5 min.

2.6. Microscopic observation

Beads in microfluidic chambers were observed under an inverted fluorescent microscope (Zeiss Axio Observer.Z1) equipped with an AxioCam 807 mono digital camera (Zeiss) and fluorescence filters using a × 10 Apochromat objective (Zeiss). Images were acquired using the 38 HE filter (excitation: BP 470/40, beam splitter: FT 495, emission: 525/50). Images were processed using the ZEN software package (Zeiss) and ImageJ. Three areas were defined in the inlet, excluding air bubbles or artifacts that could skew the measurement. The mean intensity of these areas (the sum of each pixel's intensity divided by the number of pixels in the selection) was measured using Fiji (https://imagej.net/software/fiji/). To eliminate background staining, three areas without beads were also measured. The signal intensity was calculated by subtracting the background mean from the bead areas mean as shown Fig. S3.

2.7. Detection system verification

Validation of the oligos and setup was performed with a complementary short single-strand target DNA (tDNA) corresponding to the *mecA* gene sequence that hybridizes to the arms of the new Padlock Probe (Table S1). A segment of the *vanA* gene (accession number: NG_048325.1), encoding the resistance to vancomycin which is the antibiotic used against MRSA, named ntDNA, was used as a negative control. We selected a part of the *vanA* sequence having a melting temperature equivalent to tDNA (Table S1). The complementarity of tDNA and ntDNA with the Padlock Probe is presented in Fig. S4 and their experimental validation was performed with all reactants in excess (10 µM tDNA or ntDNA, 0.25 µM Biotin-primer and 0.25 µM Padlock Probe).

2.8. System condition optimization

The impact of the Padlock Probe and Biotin-primer concentration was determined using 10 µM tDNA and 0.1 µM, 0.175 µM, and 0.25 µM of Biotin-primer with a fixed concentration of Padlock Probe (0.25 µM) or 0.25 µM, 0.3 µM, and 0.35 µM of Padlock Probe with a fixed Biotin-primer concentration (0.1 µM). Then the optimal concentrations of Padlock Probe and Biotin-primer were validated by detection of 200 ng of gDNA from *S. aureus* JE2.

2.9. Calibration curve

To obtain calibration curve, gDNA extracted from *S. aureus* JE2 in a range of concentrations from 0.2 ng to 200 ng per capture solution (25 µL) were tested under the optimized assay conditions. Two hundred nanograms of gDNA from *S. aureus* RN-R were used as a negative control, while 25 µL PBS was used as a no-template control.

2.10. PCR assay

The presence of *mecA* in clinical isolates was tested by PCR using primers mecAF and mecAR (Table S1). The assay was performed using the FIREPol DNA Polymerase Kit (Solis BioDyne, France). The reaction mix was composed of the FIREPol buffer BD X1, 2.5 mM $MgCl_2$, 0.2 mM dNTP, 0.3 µM of each primer, 0.05 U/µL of FIREPol, and 100 ng of gDNA, for a total volume of 20 µL. The thermocycler Nexus GX2 (Eppendorf, France) was programmed for a first denaturation step at 95 °C for 4 min, followed by 35 cycles of denaturation at 95 °C for 17 s, annealing at 60 °C for 35 s and extension at 72 °C for 1 min. The final extension was performed at 72 °C for 10 min. The PCR products were loaded onto 1.8 % agarose gel containing ethidium bromide solution (Invitrogen, France) and run in an electrophoresis unit (Mupid One, Eurogentec) at 135 V for 30 min. The gel was visualized using an *E*-Box Gel documentation (Vilber).

2.11. mecA gene detection in real samples

The screening of clinical *S. aureus* strains was performed using 100 ng of gDNA extracted from each isolate.

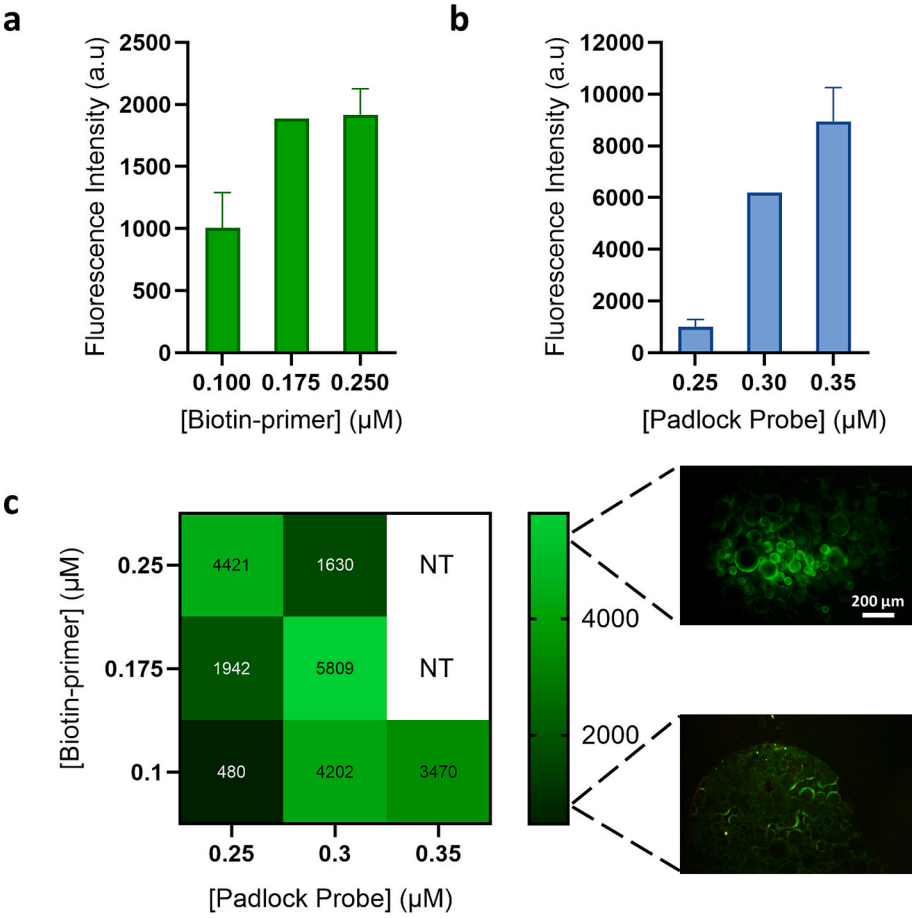

Fig. 3. Optimization of the Padlock Probe-RCA reaction. (**a**) Biosensor responses for 10 µM tDNA and 0.25 µM Padlock Probe with different concentrations of the Biotin-primer. Data points are the mean values obtained in 2 independent experiments ± SD. (**b**) Biosensor responses for detection of 10 µM tDNA, 0.1 µM Biotin-primer, and different concentrations of the Padlock Probe. Data points are the mean values obtained in 2 independent experiments ± SD. (**c**) Study of fluorescent intensity for the detection of 200 ng of gDNA from the *S. aureus* JE2 strain using various concentrations of Biotin-primer and Padlock Probe. NT: Not Tested. On the right, representative images of streptavidin beads within the reaction channel are shown for weak and strong labeling conditions: 0.3 µM Padlock Probe, 0.175 µM Biotin-primer; and 0.25 µM Padlock Probe, 0.1 µM Biotin-primer. Exposure time was 5 s.

The effect of complex biological matrix on fluorescent assay performances was studied using milk (Auchan, France), adult bovine serum (CliniSense, France) and green salad (local market, France) because they are natural biotopes for *S. aureus* and are involved in the spreading of the *mecA* gene [33]. Milk was prepared by dissolving 5 g of nonfat dry milk in 45 mL milliQ water. Serum was used without any treatment. About 50 g of pre-washed commercial salad mix was placed in a sterile container submerged in 250 mL of milliQ water and gently mixed for 15 min at room temperature. Following incubation, the salad was removed, and the water was collected, and referred to as rinse salad water, as previously explained [36]. *S. aureus* JE2 cells from an overnight culture were collected, washed three times with TES buffer and used to spike three real samples at the final concentration of 10^8 CFU/mL.

Bacterial cells were resuspended in these media and incubated under gentle agitation at room temperature for 1 h. The solutions (1-mL aliquots) were tested in the microfluidic device using three different procedures: (i) direct detection in the complex medium on lysates obtained by mechanical disruption using the FastPrep-24 kit; (ii) detection in bacterial lysates obtained after washing the cells with TES buffer followed by centrifugation; or (iii) detection after gDNA extraction and purification using the DNeasy Blood and Tissue kit. The same protocol was applied using *S. aureus* RN-R as a negative control.

2.12. Statistical analysis

All data are presented as mean ± standard deviation (SD) from at least three independent technical replicates ($n = 3$). Comparisons between two groups were performed using Student's *t*-test. Least squares regression analysis was performed to fit calibration curve using the following parameter: nonlinear regression, considering each replicate Y value as an individual point, and excluding 0 pg value. All statistical analyses were performed using GraphPad Prism software (version 10).

3. Results

3.1. Microfluidic biosensor design and operation

The microfluidic device contained 32 reaction chambers of 100 µm height (Fig. 1a, blue) and cross-channels of 20 µm height (Fig. 1a, gray). Reaction chambers were loaded with streptavidin agarose beads (average diameter 35 µm) using a pipette tip at the inlet A (Fig. 1 and Video 1). The different heights of the chamber and cross-channel stacked the beads, preventing their down-stream passage during the assay. The flow of a buffer through the cross-channel connecting the inlet B and the outlet C was measured using a syringe attached to the device via a stainless-steel catheter coupler and a polyethylene capillary pipe. The syringe pre-filled with PBS was mounted on a syringe pump that regulated the flow rate by applying a negative pressure at the outlet C

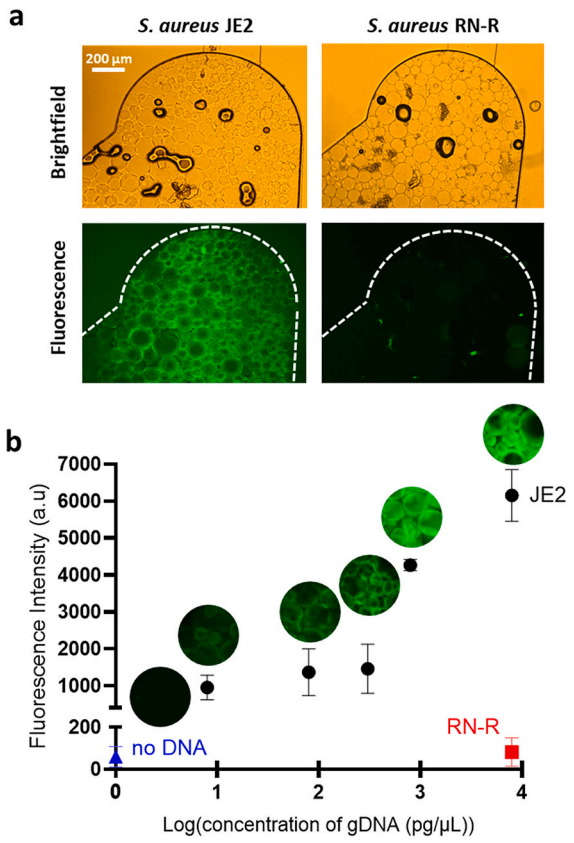

Fig. 4. Calibration curve obtained by testing different concentrations of gDNA from *S. aureus* JE2 strain (*mecA* positive) and *S. aureus* RN-R strain (*mecA* negative). (**a**) Representative optical and fluorescent images acquired for microfluidic experiments performed with two bacterial DNAs with 5 s exposure time. (**b**) Corresponding calibration curves were obtained by plotting fluorescent intensity as a function of gDNA template concentrations. Measurements were performed in PBS using purified gDNA. Data points are the mean values obtained in 3 independent experiments ± SD. Inserts are representative images of the fluorescence for each gDNA concentration.

(Fig. S2). All assay steps were performed at 37 °C, the temperature within the working temperature range of the bacteriophage Φ29 DNA polymerase that catalyzes the gene amplification [5].

The principle of the Padlock Probe-RCA method for *mecA* detection on the beads is described in Fig. 1b. Initially, a mixture containing the Padlock Probe, Biotin-primer and the target DNA is injected into the reaction channel filled with streptavidin-coated beads, using a pipette tip at the inlet A. The middle region of the Padlock Probe backbone hybridizes with the 3′-end of the Biotin-primer, while its arms hybridize with the target DNA, as illustrated in Fig. 1b and Fig. S4. The formed structure crosslinks to beads via a biotin-streptavidin bond. Thereafter, T4 ligase and ATP are injected to allow circularization of the Padlock Probe, which occurs only in the presence of the target DNA. The amplification of the Padlock Probe occurs on this circular structure after the addition of Φ29-polymerase. Finally, amplification is detected when the FAM-probe, complementary to the Rolling Circle Product (RCP), is injected. To prevent background staining that may originate from the free FAM-probe, the PBS flow is maintained for 15 min before visualization. Notably, all reaction steps are carried out in a cascade within the microfluidic device, indicating the great potential to be fully automated.

The new Padlock detection probe in the RCA assay was designed to target a highly prevalent *mecA* gene in MRSA [23]. The designed sequence (Fig. S4) was evaluated for specificity using a BLAST search, which confirmed its high specificity for the *mecA* target within the *Staphylococcus* genus.

3.2. Detection system verification

To validate the oligos and setup, the reaction was performed using tDNA and ntDNA. After completing the reactions, a microscopic examination of the microfluidic channels revealed fluorescent staining of the beads at the outer rim, which occurred exclusively in the presence of tDNA. No visible fluorescence was detected on beads with ntDNA or in controls without DNA (Fig. 2a). These results confirmed the specificity of the Padlock Probe for the detection of the *mecA* gene.

Although a clear difference between positive and negative samples was observed, beads with tDNA showed spatial variability in fluorescent intensity (Fig. 2a). This can be attributed to beads washing and solution exchange via a single negative pressure along the center line of the cross-channel. Besides, not all beads were of the same size, and larger beads showed intense outer rim labeling while their cores reminded dark (Fig. S3). To enable comparison of fluorescent intensities across experiments, fluorescence was measured on beads near the assay inlet and in several distinct areas, as illustrated in Fig. S3. The quantification of the fluorescence intensities in Fig. 2a indicated a 20-fold higher fluorescence intensity in the positive sample, compared to the background signal (Fig. 2b).

3.3. System condition optimization

Once the effectiveness of the Padlock Probe-RCA microfluidic device was verified, concentrations of the Biotin-primer and Padlock Probe, were optimized to obtain a sensitive, repeatable, and affordable platform. As expected, the increase in concentrations of both Padlock Probe and Biotin-primer enhanced the amplification efficiency and its resulting fluorescent signal, as shown in Fig. 3a and b, respectively. However, this also increased the overall cost of the test. Therefore, to find a compromise operating condition, we repeated the reaction using a gDNA from the *mecA*-positive *S. aureus* JE2 strain. Indeed, the amplification of a gene within a double-stranded DNA is always more challenging than the amplification of a short single-stranded sequence. The signal obtained for the detection of 200 ng gDNA with 0.175 µM of Biotin-primer and 0.3 µM of Padlock Probe represented the best compromise between sensitivity and cost-effectiveness of the analysis (Fig. 3c). These concentrations together with the previously optimized concentration of dNTPs and enzyme, flow rate, and reaction time [7,8] were selected for the rest of the work.

3.4. Standard curve preparation

To investigate the analytical performances of this microfluidic sensor, a calibration curve was generated using *S. aureus* JE2 gDNA over a concentration range from 8 pg/µL and 8 ng/µL. Microscopic observation revealed intense fluorescence labeling of the beads with JE2 gDNA, whereas no noticeable staining was observed with RN-R gDNA (Fig. 4a). After quantifying the data-sets obtained with a 5 s exposure time, it suggested a nonlinear increment ($y = 1828\times\text{-}1578$, $R^2 = 0.77$) of fluorescence intensities with a high degree of positive correlation between fluorescent intensity and concentrations of JE2 gDNA (Fig. 4b). To verify whether the nonlinearity originated from the saturation of the fluorescence at higher gDNA concentrations, the staining of beads was quantified for different exposure time (1 s – 5 s). This analysis indicated a linear increase in signal intensity with function of exposure time, which excludes signal saturation (Fig. S5). We may speculate that the nonlinear regression curve reflects the polydispersity of the commercial streptavidin beads used (Fig. S4). The experimental limit of detection was 8 pg/µL, which corresponds to 0.2 ng of gDNA per reaction. Considering that we flowed 20 µL of reaction mixture, and that there is only one copy of *mecA* per gDNA, we can estimate the experimental limit to be about 10^4 *S. aureus* cells per reaction.

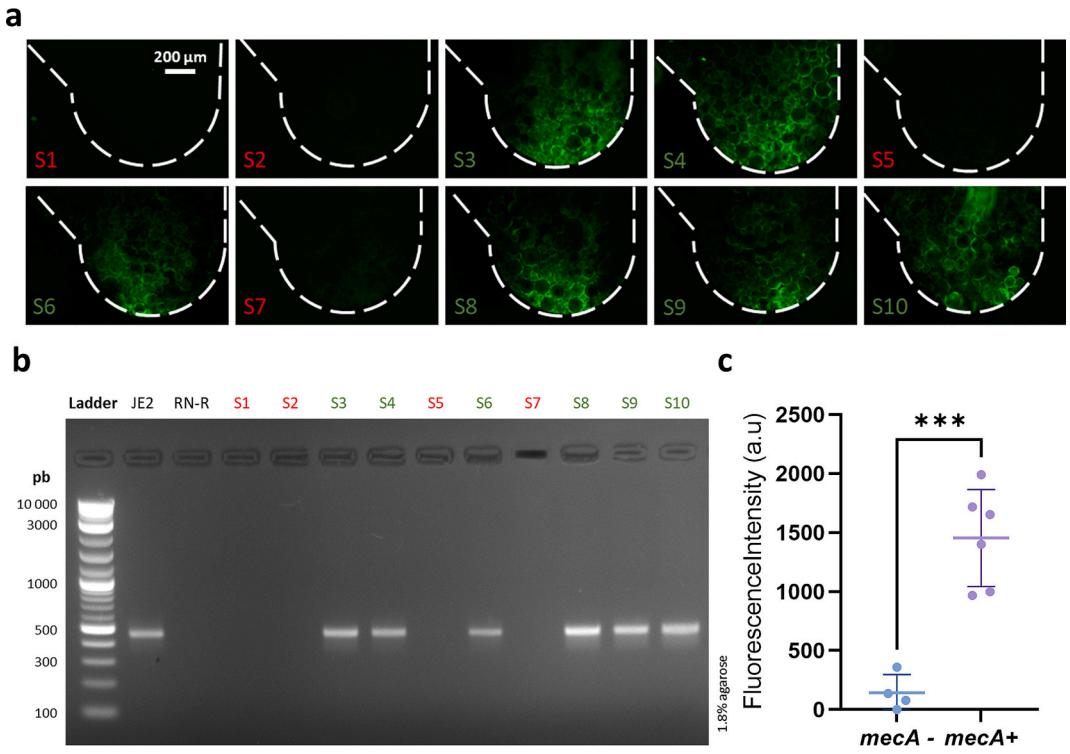

Fig. 5. Selectivity study performed with purified gDNA from clinical *S. aureus* strains related to sepsis. (**a**) Representative images comparing fluorescent signal intensities obtained with *mecA*-positive and *mecA*-negative strains. (**b**) PCR analysis with primers mecAF and mecAR, confirming results obtained with the microfluidic device in (**a**). PCR was performed with 100 ng of gDNA from each clinical strain and with *S. aureus* JE2 and RN-R as positive and negative controls, respectively. PCR products were run on a 1.8 % agarose gel electrophoresis. (**c**) Statistical analysis was conducted on fluorescent intensities measured for clinical strains using the microfluidic Padlock Probe-RCA analysis. Results show the average and range of biologically independent samples. *P*-values were determined by Student-*t*-test (*** < 0.0002).

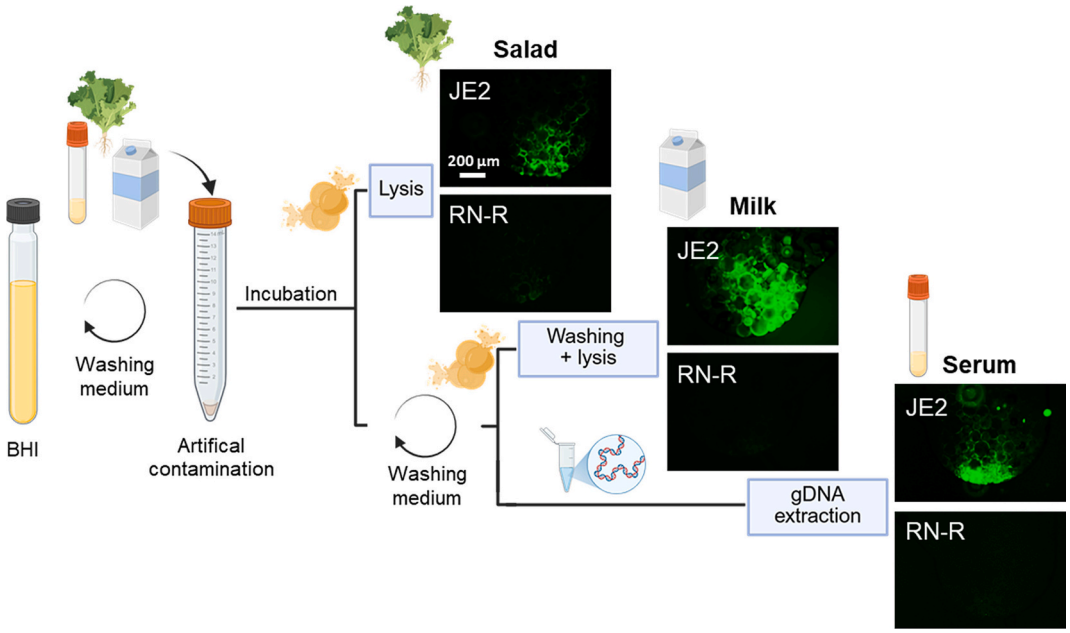

Fig. 6. Detection of *mecA* in complex biological samples using the microfluidic device. An overnight culture of *S. aureus* JE2 was used to artificially contaminate milk, serum, and green salad rinsing water. First, an aliquot of each medium was lysed and tested. The *mecA* gene was successfully detected only in the green salad rising water. Second, the bacterial cells were washed with TES buffer and then lysed. This protocol enabled the detection of the *mecA* gene in the milk sample. Finally, bacterial gDNA was extracted and purified, and then tested. This protocol enabled the detection of the *mecA* gene in serum. More representative results are presented in Fig. S6. (For interpretation of the references to colour in this figure legend, the reader is referred to the web version of this article.)

3.5. Clinical sample testing

To test the medical relevance and potential, the assay performance was evaluated in PBS solution in the presence of *S. aureus* clinical isolates related to sepsis (Fig. 5a). The results were compared to a PCR analysis with *S. aureus* JE2 and RN-R strains as a positive and negative control, respectively (Fig. 5b). As shown in Fig. 5a and b, fluorescent staining was observed exclusively in *S. aureus* strains that tested positive for the *mecA* gene by PCR. The statistical analysis demonstrated that the fluorescent signal variation observed with *mecA*-positive strains was significantly different from that observed with *mecA*-negative strains (p-value <0.0002), indicating that the signal intensity clearly distinguishes positives from negatives samples. These results further support the selectivity of this microfluidic assay, and confirm the specificity of the newly designed Padlock Probe. In contrast to PCR which typically requires expensive and bulky thermal cyclers and long reaction times lasting several hours, our assay overcomes these limitations, offering a convenient and rapid approach for in vitro clinical diagnostics.

3.6. Testing of three practical samples

Next, to evaluate sensor performance in complex biological samples relevant to cases such as mastitis, sepsis, and food contamination, biotope-induced background responses were tested using spiked milk, serum, and green salad rinsing water (see Materials and Methods for details). When bacterial cells were mechanically broken directly in these media without cell prewashing, direct visualization of the *mecA* gene was observed in the salad rinsing water (Fig. 6). However, no staining was observed in milk and serum samples (Fig. S6). We speculated that in milk and serum either the matrix turbidity prevents reaction and visualization of results, or molecules in these media inhibit amplification. Indeed, the flow can be blocked with the protein-rich milk samples. Therefore, we washed the bacterial cells with TES buffer before lysis and performed the test. The prewashing enabled *mecA* detection in JE2 from milk (Fig. 6). Given that milk is rich in proteins prone to forming aggregates, rinsing the cells before analysis likely removed these larger particles, thereby enabling unobstructed flow of the solution through the microfluidic system. However, fluorescence was not observed in prewashed bacterial cells from serum (Fig. S6), suggesting that serum molecules bound to cells inhibited the amplification. Indeed, molecules such as hemoglobin or immunoglobulin G in serum are recognized as potent PCR inhibitors, as they impair the catalytic activity of DNA polymerase and thereby reduces amplification efficiency [38]. These molecules may also inhibit Φ29 DNA Polymerase used here. Nevertheless, when gDNA of *S. aureus* cells in serum was extracted and purified by a commercial kit, the isothermal amplification of the *mecA* gene by the Padlock Probe-RCA was efficient (Fig. 6 and Fig. S6). Across all experiments in Fig. 6, the control *S. aureus* RN-R strain exhibited no staining.

4. Discussion

Nucleic acids are essential biomarkers in medical diagnostics, agri-food analysis, and environmental monitoring. Over the past decades, various isothermal amplification-based nucleic acid detection methods have been developed and optimized. Among them, RCA is particularly well-suited for biosensor development due to its simplicity and high efficiency. RCA operates at relatively low temperatures (30–40 °C), which can be maintained by body heat, allowing the assay to be performed without an external heating device [4,16]. In contrast to polymerase/recombinase-based amplification methods such as PRA or RAA, which also function at low temperatures (37–42 °C), RCA produces minimal background signal, as demonstrated in this study. Furthermore, Padlock Probe-mediated RCA enables the amplification of target genes into long-chain DNA products that can be readily detected without specialized equipment or the complex operational steps required by traditional isothermal methods such as LAMP [42]. Moreover, the use of the Biotin- primer ensured the binding of amplicons to the streptavidin beads, thereby reducing nonspecific hybridization and improving both the sensitivity and selectivity of detection.

The device used in this study, composed of 32 independent reaction chambers, provides a possibility to analyze 32 samples in parallel within the same chip with a high reproducibility. The combination of isothermal amplification with a microfluidic device enabled rapid and straightforward direct detection of the *mecA* gene in water used for salad washing. In the more complex milk matrix, direct detection was also possible but required a pre-washing step to remove protein aggregates. Finally, amplification of the *mecA* gene from *S. aureus* in serum required extraction of bacterial gDNA, likely due to the presence of DNA polymerase inhibitors in this medium. Based on the experimental data, the limit of detection was estimated at 10^4 cells, which is well below the reported infectious dose for *S. aureus* 10^5 cells and $> 10^{10}$ cells when ingested [19,25,34], confirming the applicability of the microfluidic device to real samples. The potential of our device for Point-of-Care testing also lies in its simple microfluidic design, in which fluid manipulation is achieved by applying negative pressure rather than by using centrifugal force, as in most studies [16,40,41].

5. Conclusion

In summary, we successfully developed a microfluidic device for sensitive and specific detection of the *mecA* gene in biological matrices. The platform is based on an RCA isothermal amplification with a new Padlock Probe designed to recognize the target *mecA* gene. Moreover, when the assays were performed with clinical blood isolates of *S. aureus* associated with sepsis, the fluorescent read-out allowed the identification of *mecA*-positive stains with 100 % of sensitivity. Given its low cost, rapidity and simplicity of design, this sensor represents a promising alternative to trace and detect genes responsible for antibiotic resistance. In the future portable and automatized detection of bacteria carrying resistance genes could enable faster diagnostics, tailor antibiotic treatment and ultimately prevent antibiotic resistance spreading.

Supplementary data to this article can be found online at https://doi.org/10.1016/j.sbsr.2025.100941.

Novelty statement

This manuscript has not been published or presented elsewhere in part or in entirety and is not under consideration by another journal. We have read and understood your journal's policies, and we believe that neither the manuscript nor the study violates any of these. There are no conflicts of interest to declare.

CRediT authorship contribution statement

Léo Baldenweck: Writing – review & editing, Writing – original draft, Visualization, Validation, Methodology, Investigation, Formal analysis, Data curation. **Catarina Caneira:** Writing – review & editing, Methodology, Investigation. **Jasmina Vidic:** Writing – review & editing, Writing – original draft, Supervision, Project administration, Funding acquisition.

Declaration of competing interest

The authors declare that they have no known competing financial interests or personal relationships that could have appeared to influence the work reported in this paper.

Acknowledgements

This work was supported by the European Union under grant agreements N° 872662 (IPANEMA project) and N° 101135402 (MOBILES project, to JV). Léo Baldenweck acknowledges the Graduate

School Biosphera for the Mobility Grant BSE-2025-47. Catarina Caneira acknowledges funding from Fundação para a Ciência e a Tecnologia (FCT) for the Plurianual financing of the Research Unit INESC MN (UID/PRR/5367) and through i4HB-Laboratório Associado (LA/P/140/2020).

The authors thank Dr. Narayanan S. Madaboosi and Shrishti Kumari (Indian Institute of Technology Madras) for in silico evaluating the Padlock Probe, Prof. João P. Conde and Dr. Virginia Chu (INESC-MN) and Dr. Sandrine Truchet (INRAE) for their support and stimulating discussions.

Data availability

The data are available in the Supplementary Information.

References

[1] W.A. Al-Soud, P. Rådström, Purification and characterization of PCR-inhibitory components in blood cells, J. Clin. Microbiol. 39 (2) (2001) 485–493.
[2] S.S. Ambade, V.K. Gupta, R.P. Bhole, P.B. Khedekar, R.V. Chikhale, A review on five and six-membered heterocyclic compounds targeting the penicillin-binding protein 2 (PBP2A) of methicillin-resistant *Staphylococcus aureus* (MRSA), Molecules 28 (20) (2023) 7008.
[3] N. Arulkumaran, M. Routledge, S. Schlebusch, J. Lipman, A. Conway Morris, Antimicrobial-associated harm in critical care: a narrative review, Intensive Care Med. 46 (2) (2020) 225–235.
[4] R.M. Bialy, A. Mainguy, Y. Li, J.D. Brennan, Functional nucleic acid biosensors utilizing rolling circle amplification, Chem. Soc. Rev. 51 (21) (2022) 9009–9067.
[5] L. Blanco, M. Salas, Characterization and purification of a phage phi 29-encoded DNA polymerase required for the initiation of replication, Proc. Natl. Acad. Sci. 81 (17) (1984) 5325–5329.
[6] S.T. Calzuola, G. Newman, T. Feaugas, C.M. Perrault, J.-B. Blondé, E. Roy, J. Vidic, Membrane-based microfluidic systems for medical and biological applications, Lab Chip 24 (15) (2024) 3579–3603.
[7] C.R. Caneira, R.R. Rosa, V. Chu, M. Nilsson, N. Madaboosi, R.R. Soares, J.P. Conde, A systematic implementation of padlock probing-based rolling circle amplification in an integrated microfluidic device for quantitative biomolecular analyses, Anal. Chim. Acta 1351 (2025) 343834.
[8] C.R. Caneira, R.R. Soares, K. Nikolaidou, M. Nilsson, N. Madaboosi, V. Chu, J. P. Conde, Rolling circle amplification in bead-based microfluidic device with integrated photodiode for fluorescence signal transduction, in: 2021 IEEE 34th International Conference on Micro Electro Mechanical Systems (MEMS), IEEE, 2021, pp. 575–578.
[9] J. Cottet, P. Renaud, Introduction to microfluidics, in: Drug Delivery Devices and Therapeutic Systems, Elsevier, 2021, pp. 3–17.
[10] E.M. Darby, E. Trampari, P. Siasat, M.S. Gaya, I. Alav, M.A. Webber, J.M. Blair, Molecular mechanisms of antibiotic resistance revisited, Nat. Rev. Microbiol. 21 (5) (2023) 280–295.
[11] S. De Silva, S.-S. Lee, M.B. Dugan, J.L. Anderson, Recent advancements and emerging techniques in nucleic acid isolation, amplification, and detection from diverse complex matrices of human interest, TrAC Trends Anal. Chem. 118172 (2025).
[12] M. Djisalov, L. Janjušević, V. Léguillier, L. Šašić Zorić, C. Farre, J. Anba-Mondoloni, I. Gadjanski, Loop-mediated isothermal amplification (LAMP) assay coupled with gold nanoparticles for colorimetric detection of Trichoderma spp. Agaricus bisporus cultivation substrates, Sci. Rep. 14 (1) (2024) 15539.
[13] P.D. Fey, J.L. Endres, V.K. Yajjala, T.J. Widhelm, R.J. Boissy, J.L. Bose, K. W. Bayles, A genetic resource for rapid and comprehensive phenotype screening of nonessential *Staphylococcus aureus* genes, MBio 4 (1) (2013) 00537-00512, https://doi.org/10.1128/mbio.
[14] K. Gibson, K. Schwab, S. Spencer, M. Borchardt, Measuring and mitigating inhibition during quantitative real time PCR analysis of viral nucleic acid extracts from large-volume environmental water samples, Water Res. 46 (13) (2012) 4281–4291.
[15] L. He, X. Yu, R. Huang, L. Jin, Y. Liu, Y. Deng, Z. Li, A novel specific and ultrasensitive method detecting extracellular vesicles secreted from lung cancer by padlock probe-based exponential rolling circle amplification, Nano Today 42 (2022) 101334.
[16] Y. Hou, Z. Liu, H. Huang, C. Lou, Z. Sun, X. Liu, W. Zhou, Biosensor-based microfluidic platforms for rapid clinical detection of pathogenic Bacteria, Adv. Funct. Mater. 35 (1) (2025) 2411484.
[17] B.P. Howden, S.G. Giulieri, T. Wong Fok Lung, S.L. Baines, L.K. Sharkey, J.Y. Lee, T.P. Stinear, Staphylococcus aureus host interactions and adaptation, Nat. Rev. Microbiol. 21 (6) (2023) 380–395.
[18] K.S. Ikuta, L.R. Swetschinski, G.R. Aguilar, F. Sharara, T. Mestrovic, A.P. Gray, A. G. Hayoon, Global mortality associated with 33 bacterial pathogens in 2019: a systematic analysis for the global burden of disease study 2019, Lancet 400 (10369) (2022) 2221–2248.
[19] S. Jankie, J. Jenelle, R. Suepaul, L.P. Pereira, P. Akpaka, A.S. Adebayo, G. Pillai, Determination of the infective dose of *Staphylococcus aureus* (ATCC 29213) and *Pseudomonas aeruginosa* (ATCC 27853) when injected intraperitoneally in Sprague Dawley rats, Br. J. Pharm. Res. 14 (1) (2016) 1–11.
[20] S.P. Jonstrup, J. Koch, J. Kjems, A microRNA detection system based on padlock probes and rolling circle amplification, Rna 12 (9) (2006) 1747–1752.
[21] S.R. Krishnan, R.R. Soares, N. Madaboosi, M.M. Gromiha, AutoPLP: a padlock probe design pipeline for zoonotic pathogens, ACS Infect. Dis. 9 (3) (2023) 459–469.
[22] A.S. Lee, H. De Lencastre, J. Garau, J. Kluytmans, S. Malhotra-Kumar, A. Peschel, S. Harbarth, Methicillin-resistant *Staphylococcus aureus*, Nat. Rev. Dis. Primers 4 (1) (2018) 1–23.
[23] V. Léguillier, D. Pinamonti, C.-M. Chang, R. Mukherjee, A. Cossetini, M. Manzano, J. Vidic, A review and meta-analysis of *Staphylococcus aureus* prevalence in foods, The Microbe 4 (2024) 100131.
[24] H. Liu, L. Li, L. Duan, X. Wang, Y. Xie, L. Tong, B. Tang, High specific and ultrasensitive isothermal detection of microRNA by padlock probe-based exponential rolling circle amplification, Anal. Chem. 85 (16) (2013) 7941–7947.
[25] M. Marin, F. Rizzotto, V. Léguillier, C. Péchoux, E. Borezee-Durant, J. Vidic, Naked-eye detection of *Staphylococcus aureus* in powdered milk and infant formula using gold nanoparticles, J. Microbiol. Methods 201 (2022) 106578.
[26] M. Moreira, D. Adamoski, J. Sun, M.J. Najafzadeh, M.M.F.D. Nascimento, R. R. Gomes, V.A. Vicente, Detection of *Streptococcus mutans* using padlock probe based on rolling circle amplification (RCA), Braz. Arch. Biol. Technol. 58 (2015) 54–60.
[27] M. Naghavi, S.E. Vollset, K.S. Ikuta, L.R. Swetschinski, A.P. Gray, E.E. Wool, C. Han, Global burden of bacterial antimicrobial resistance 1990–2021: a systematic analysis with forecasts to 2050, Lancet 404 (10459) (2024) 1199–1226.
[28] M. Nilsson, H. Malmgren, M. Samiotaki, M. Kwiatkowski, B.P. Chowdhary, U. Landegren, Padlock probes: circularizing oligonucleotides for localized DNA detection, Science 265 (5181) (1994) 2085–2088.
[29] H.T. Nour El-Din, A.S. Yassin, Y.M. Ragab, A.M. Hashem, Phenotype-genotype characterization and antibiotic-resistance correlations among colonizing and infectious methicillin-resistant *Staphylococcus aureus* recovered from intensive care units, Infect. Drug Resist. (2021) 1557–1571.
[30] A. Pathania, J. Anba-Mondoloni, M. Gominet, D. Halpern, J. Dairou, L. Dupont, A. Gruss, ppGpp/GTP and malonyl-CoA modulate *Staphylococcus aureus* adaptation to FASII antibiotics and provide a basis for synergistic bi-therapy, MBio 12 (1) (2021) 03193-03120, https://doi.org/10.1128/mbio.
[31] S.J. Peacock, G.K. Paterson, Mechanisms of methicillin resistance in *Staphylococcus aureus*, Annu. Rev. Biochem. 84 (1) (2015) 577–601.
[32] D. Pinamonti, M. Manzano, M. Maifreni, S. Bianco, B. Domi, A. Ferrin, J. Vidic, Prevalence and characterization of *Staphylococcus aureus* isolated from meat and milk in northeastern Italy, J. Food Prot. 88 (2) (2025) 100442.
[33] D. Pinamonti, J. Vidic, M. Maifreni, A. Cossettini, V. Leguillier, M. Manzano, Water-mediated dissemination and detection of antibiotic resistance across livestock, Agri-food, and aquaculture systems, Micromachines 16 (8) (2025) 934.
[34] P. Schmid-Hempel, S.A. Frank, Pathogenesis, virulence, and infective dose, PLoS Pathog. 3 (10) (2007) e147.
[35] C. Schrader, A. Schielke, L. Ellerbroek, R. Johne, PCR inhibitors–occurrence, properties and removal, J. Appl. Microbiol. 113 (5) (2012) 1014–1026.
[36] M. Sentic, F. Rizzotto, Z. Novakovic, A. Karajic, B. Heddi, J. Vidic, Improving electrochemical aptasensor sensitivity for *Bacillus cereus* spore detection in food safety applications, Talanta 299 (2026) 129147.
[37] Z. Shao, J. Zhang, Z. Jin, F. Qu, C. Du, Y. Ming, L. He, Machine learning-enabled microfluidic ratiometric fluorescence sensor array based on lanthanide-gold nanoclusters for visual detection of multicomponent antibiotics, Biosens. Bioelectron. 118109 (2025).
[38] M. Sidstedt, J. Hedman, E.L. Romsos, L. Waitara, L. Wadsö, C.R. Steffen, P. Rådström, Inhibition mechanisms of hemoglobin, immunoglobulin G, and whole blood in digital and real-time PCR, Anal. Bioanal. Chem. 410 (10) (2018) 2569–2583.
[39] R.R. Soares, J.C. Varela, U. Neogi, S. Ciftci, M. Ashokkumar, I.F. Pinto, A. Russom, Sub-attomole detection of HIV-1 using padlock probes and rolling circle amplification combined with microfluidic affinity chromatography, Biosens. Bioelectron. 166 (2020) 112442.
[40] J. Vidic, P. Vizzini, M. Manzano, D. Kavanaugh, N. Ramarao, M. Zivkovic, I. Gadjanski, Point-of-need DNA testing for detection of foodborne pathogenic bacteria, Sensors 19 (5) (2019) 1100.
[41] G. Xing, W. Zhang, N. Li, Q. Pu, J.-M. Lin, Recent progress on microfluidic biosensors for rapid detection of pathogenic bacteria, Chin. Chem. Lett. 33 (4) (2022) 1743–1751.
[42] J. Zhuang, Z. Zhao, K. Lian, L. Yin, J. Wang, S. Man, L. Ma, SERS-based CRISPR/Cas assay on microfluidic paper analytical devices for supersensitive detection of pathogenic bacteria in foods, Biosens. Bioelectron. 207 (2022) 114167.